Structure of the three-point correlation function of a passive scalar in the presence of a mean gradient

Alain Pumir
Institut Nonlinéaire de Nice, CNRS, 1361 route des Lucioles, F-06560 Valbonne, France
(Received 1 October 1997)

The three-point correlation function of a passive scalar advected by a random, incompressible velocity field in the presence of a mean gradient is investigated by means of phenomenological Hopf equations. Numerical solutions are provided in the case where the velocity is Gaussian, white in time, and with a power law in space, $\langle[v(\vec{r})-v(\vec{0})]^2\rangle \sim r^{2-\epsilon}$, and in the model introduced by Shraiman and Siggia [C. R. Acad. Sci. **321**, 279 (1995)]. Anomalous scaling exponents are found in both models. The numerics agrees with all the available analytic, perturbative results. In addition, the angular dependence of the correlation function is explicitly determined. In the Batchelor limit of random advection by a smooth velocity field, the exponent is found to remain very close to 1, as found experimentally. In this limit, the three-point correlation function is found to be very well represented, away from collinearity, by an explicit integral representation. [S1063-651X(98)05103-4]

PACS number(s): 47.10.+g, 47.27.−i

I. INTRODUCTION

Mixing is one of the most important properties of a turbulent flow. The problem can be simply formulated by considering a passive scalar Θ, which evolves according to the advection-diffusion equation

$$\partial_t \Theta + (\vec{u}\cdot\vec{\nabla})\Theta = \kappa\nabla^2\Theta, \tag{1}$$

where $\vec{u}$ is the turbulent velocity field. The passive scalar therefore probes the velocity field, so its statistical properties have a number of similarities to those of the turbulent velocity field itself [1]. In particular, the Kolmogorov theory [2,3] can be extended to the scalar [4,5]. Although the spectrum of scalar fluctuations shows a convincing $k^{-5/3}$ range [6], the higher-order correlation function do not follow the predictions of the Kolmogorov theory [1,7]. Significant departures are observed already at the level of the three-point correlation function. In heated boundary layers, for example, the scalar derivative skewness $s \equiv \langle(\partial_x\Theta)^3\rangle/\langle(\partial_x\Theta)^2\rangle^{3/2}$ (x is the coordinate in the downstream direction) remains of order 1, essentially independent of the Reynolds number [1,8]. In this flow, the shear induced near the wall breaks the $x \to -x$ symmetry, allowing a nonzero three-point correlation function. It was also found that the structure function $\langle[\Theta(x)-\Theta(0)]^3\rangle$ behaves linearly with x [9], whereas arguments based on Kolmogorov's phenomenology would rather suggest a $x^{5/3}$ dependence. These results imply that the anisotropy present at large scales has a strong influence all the way down to small scales.

The scalar derivative skewness was also observed to remain of order 1 in the simpler problem of mixing of a passive scalar by a homogeneous isotropic turbulent flow, in the presence of an imposed scalar gradient [10–12]. We focus here on the latter problem and denote by $\hat{G}$ the scalar gradient ($|\hat{G}|=1$) and by θ the scalar fluctuation $\Theta = \theta + G\cdot\vec{r}$, so Eq. (1) becomes

$$\partial_t\theta + (\vec{u}\cdot\vec{\nabla})\theta = \kappa\nabla^2\theta - \hat{G}\cdot\vec{u}. \tag{2}$$

The gradient introduces a forcing term, allowing one to maintain a steady state for the fluctuating scalar. We emphasize that in this problem, the symmetries impose that the three-point correlation function is *odd* in space.

Interestingly, the effect does not seem to depend on the precise statistical properties of the flow: A Gaussian random velocity field with an inertial range scaling $\langle[v(\vec{r})-v(\vec{0})]^2\rangle \sim \vec{r}^{2/3}$ is enough to obtain a scalar derivative skewness independent of the Péclet number [11]. This remark suggests that much can be learned about these issues with the help of simplified models. We focus here on two simplified models.

The problem of mixing by a random Gaussian, white in time velocity field with a scaling exponent $2-\epsilon$,

$$\langle v_a(\vec{r},t)v_b(\vec{r}',t')\rangle = \delta(t-t')C_{ab}(\vec{r}-\vec{r}'), \tag{3a}$$

$$D_{ab}(\vec{r}) \equiv [C_{ab}(0)-C_{ab}(\vec{r})] = D_0\left((d+1-\epsilon)\delta_{ab} - (2-\epsilon)\frac{r^a r^b}{|\vec{r}|^2}\right)|\vec{r}|^{2-\epsilon}, \tag{3b}$$

has been introduced long ago by Kraichnan [13], who showed that the N-point correlation function $\langle\theta(\vec{r}_1)\cdots\theta(\vec{r}_N)\rangle$ obeys a closed equation of the form [14]

$$L(d,\epsilon)\langle\theta(\vec{r}_1)\cdots\theta(\vec{r}_N)\rangle = \mathrm{RHS}, \tag{4a}$$

where the operator $L(d,\epsilon)$ is defined in the inertial range by

$$L(d,\epsilon) \equiv \sum_{i\neq j}^{N} D_{ab}(\vec{r}_i-\vec{r}_j)\partial^a_{r_i}\partial^b_{r_j} \tag{4b}$$

and the right-hand side (RHS) of Eq. (4a) involves only lower-order correlation functions. Anomalous scaling exponents may be obtained as zero modes of the operator $L(d,\epsilon)$, homogeneous in space. The existence of such an eigenfunction has been established analytically in the case of an isotropic forcing and in the case of an even-order correlation

function in various limits [15,16]. In this model and in the limit where $|\vec{r}_1-\vec{r}_2|$ is much smaller than the other distances in the problem, the N-point correlation function behaves as $|\vec{r}_1-\vec{r}_2|^{\epsilon}$. In order to ensure that the correlation function behaves like $|\vec{r}_1-\vec{r}_2|^{2/3}$, as expected, one has to choose the value $\epsilon=2/3$.

A different class of models has been introduced by Shraiman and Siggia [17,18] in order to take into account the finite correlation time as a function of scale $\tau_R\sim\epsilon^{-1/3}R^{2/3}$, where ϵ is the rate of dissipation of turbulent energy. A set of points $(\vec{r}_1,\vec{r}_2,\ldots,\vec{r}_N)$ separated from each other by a distance $\sim R$ is mapped under the action of the turbulent velocity field, during a time τ_R, onto a new set of positions $(\vec{r}_1',\vec{r}_2',\ldots,\vec{r}_N')$. The main idea consists in decomposing the velocity field as a sum of (i) an essentially constant piece, due to scales much greater than R, plus (ii) a coherent strain, at scale $\sim R$, plus (iii) an incoherent part, due to the small scale jittering. The large-scale uniform piece (i) affects the N-point correlation function through the forcing term (motion in the gradient). The coherent strain (ii) corresponds to advection by a smooth, random field ($\epsilon=0$) [19], whose effect can be modeled by the Batchelor-Kraichnan operator $\mathcal{L}_0\equiv L(d,\epsilon=0)$ [Eq. (4b) with $\epsilon=0$]. The small-scale motion (iii) is the source of the eddy diffusivity and is modeled phenomenologically by a perturbation to the Batchelor-Kraichnan operator $\alpha\mathcal{L}_D$, where $\mathcal{L}_D$ is chosen here to be

$$\mathcal{L}_D=\frac{3d}{2}\,R_g^2\left(\frac{r_{12}^2r_{23}^2r_{31}^2}{R_g^6}\right)^{2/3}\nabla^2, \tag{5}$$

where $r_{ij}\equiv|\vec{r}_i-\vec{r}_j|$, $R_g^2\equiv r_{12}^2+r_{23}^2+r_{31}^2$, and α is formally a small parameter. The problem then reduces to

$$\mathcal{L}(d,\alpha)\langle\theta(\vec{r}_1)\,\theta(\vec{r}_2)\,\theta(\vec{r}_3)\rangle=\mathrm{RHS}, \tag{6a}$$

with

$$\mathcal{L}(d,\alpha)=\mathcal{L}_0+\alpha\mathcal{L}_D, \tag{6b}$$

so the existence of anomalous exponents in this model is determined by the zero modes of the operator $\mathcal{L}(d,\alpha)$. The perturbation operator is dominant when two points come close together, so in the limit $|\vec{r}_1-\vec{r}_2|\ll|\vec{r}_1-\vec{r}_3|,|\vec{r}_2-\vec{r}_3|$, $\langle\theta(\vec{r}_1)\,\theta(\vec{r}_2)\,\theta(\vec{r}_3)\rangle\gtrsim|\vec{r}_1-\vec{r}_2|^{2/3}$, therefore reproducing the behavior expected from the Kolmogorov analysis. For this reason, we refer to this model as the pseudo-Kolmogorov model, or in short the K model. The validity of this phenomenological model has to be established by direct confrontations with experimental results. For the sake of the analysis, we also considered the simpler model where the dissipation is simply the Laplacian $\mathcal{L}_D'\equiv\alpha(d/6)R_g^2\nabla^2$, which will be referred to as the L model.

The theoretical analysis of the Kraichnan model in the limit $\epsilon\to0$ [20], appropriate to understand qualitatively the case $\epsilon=2/3$, and of the K model for small values of α [17,21] rests on singular perturbation theory. It is also possible to reduce the full problem to an elliptic operator in a rectangle in two-dimensions, which can be treated numerically [22]. The purpose of this work is to analyze the solutions of the white-noise model and K model for the three-point correlation function, in the presence of a mean gradient.

Section II is devoted to a review of the necessary theoretical background, in particular, of the available information from perturbation theory. The numerical methods are explained in Sec. III. Section IV is devoted the numerical results: We discuss the scaling exponents in the Kraichnan model (Sec. IV A) and in the K model (Sec. IV B) and then various results concerning the structure of the correlation function. We briefly discuss our results in Sec. V.

II. THEORETICAL BACKGROUND

In this section we define our notation and introduce the theoretical results necessary to analyze our numerical results.

A. Notation

We begin by introducing the vectors

$$\vec{\rho}_1\equiv(\vec{r}_1-\vec{r}_2)/\sqrt{2},\quad \vec{\rho}_2\equiv(\vec{r}_1+\vec{r}_2-2\vec{r}_3)/\sqrt{6}. \tag{7}$$

With these variables, the operator $L(d,\epsilon)$ reads

$$L(d,\epsilon)\equiv\sum_{\mathcal{S}_3}|\vec{\rho}_1|^{-\epsilon}[(d+1-\epsilon)\vec{\rho}_1^2(\partial_1^a\partial_1^a-\tfrac{1}{3}\partial_2^a\partial_2^a) -(2-\epsilon)\rho_1^a\rho_1^b(\partial_1^a\partial_1^b-\tfrac{1}{3}\partial_2^a\partial_2^b)], \tag{8}$$

the summation extending over the cyclic permutations of $(\vec{r}_1,\vec{r}_2,\vec{r}_3)$ (group $\mathcal{S}_3$), which are equivalent to the transformations

$$\vec{\rho}_1\to-\frac{\vec{\rho}_1}{2}\pm\frac{\sqrt{3}}{2}\,\vec{\rho}_2,\quad \vec{\rho}_2\to\mp\frac{\sqrt{3}}{2}\,\vec{\rho}_1-\frac{\vec{\rho}_2}{2}. \tag{9}$$

The Laplacian operator in $\vec{r}$ simply becomes the Laplacian in $\vec{\rho}$.

It is convenient to express the two vectors $(\vec{\rho}_1,\vec{\rho}_2)$ as $\rho_i^a=\Sigma_{i'}R_{ii'}(\chi)\xi_{i'}\hat{\eta}_{i'}^a$. The 2×2 matrix $R(\chi)$ is the rotation matrix of angle χ in ''pseudospace.'' The two orthogonal unit vectors $\hat{\eta}_1,\hat{\eta}_2$ span the plane defined by $(\vec{\rho}_1,\vec{\rho}_2)$. It is enough to consider the variables ξ_1,ξ_2 such that $0\leqslant|\xi_1|<\xi_2$ to parametrize all the possible configurations. The area of the triangle $|\vec{\rho}_1\times\vec{\rho}_2|$ is simply equal to $\zeta=|\xi_1\xi_2|$. We also introduce the dimensionless variable $w\equiv2\xi_1\xi_2/(\xi_1^2+\xi_2^2)$ (occasionally, we also introduce $\xi=1/w$). The change of variables $(w,\zeta)\to(\xi_1,\xi_2)$ is one to one for $-1\leqslant w\leqslant1$ and $0\leqslant\mathrm{sgn}(w)\zeta\leqslant\infty$, with

$$\xi_1=\left(\frac{\zeta}{w}\right)^{1/2}(1-\sqrt{1-w^2})^{1/2},\quad \xi_2=\left(\frac{\zeta}{w}\right)^{1/2}(1-\sqrt{1-w^2})^{1/2}. \tag{10}$$

The variables w and ζ provide a convenient parametrization of the vicinity of $|\rho_1|=0$, i.e., of the region where $|\vec{r}_1-\vec{r}_2|\ll|\vec{r}_1-\vec{r}_3|,|\vec{r}_2-\vec{r}_3|$. In this region, w and χ are small, $\vec{\rho}_1\approx\xi_2(w\,\hat{\eta}_1/2+\chi\,\hat{\eta}_2)$, and $\vec{\rho}_2\approx\xi_2\hat{\eta}_2$, so $|\rho_1|^2\approx\xi_2^2(w^2/4+\chi^2)$.

The dilation operator $\Lambda \equiv \rho_i^a \partial_{\rho_i^a}$ reduces in our variables to $\Lambda = 2\zeta \partial_\zeta$. We denote by λ the scaling exponent of the solution.

B. Expression of the differential operators

The operators considered here $L(d,\epsilon)$ and $\mathcal{L}(d,\alpha)$ are invariant under rotation, so they commute with the angular momentum operators $L_{ab} = i\Sigma_j(\rho_j^a \partial_{\rho_j^b} - \rho_j^b \partial_{\rho_j^a})$ and $L^2 \equiv \frac{1}{2}\Sigma_{a,b} L_{ab} L_{ab}$. Thus one may look for zero modes with a given angular momentum l [$L^2\psi = l(l+d-2)\psi$]. Since the symmetries of the problem impose that the solution is odd in space, l must be odd. We restrict to $l=1$ and look for a solution of the form

$$\Psi \equiv \langle \theta(\vec{r}_1)\theta(\vec{r}_2)\theta(\vec{r}_3)\rangle = |\zeta|^{\lambda/2}\hat{G}\cdot[\varphi_1(\chi,w)\hat{\eta}_1 + \varphi_2(\chi,w)\hat{\eta}_2]. \quad (11)$$

The limit where the three points are aligned, $\xi_1/\xi_2 \to 0$ or, equivalently, $w \to 0$, $\zeta \to 0$, requires some care. The correlation function reduces to a homogeneous function of ξ_2, of degree λ. This suggests that when $w \to 0$, $\varphi_1, \varphi_2 \sim |w|^{-\lambda/2}$. For this reason, we introduce $\phi_i \equiv |w|^{\lambda/2}\varphi_i$, so

$$\Psi = \left(\frac{\zeta}{w}\right)^{\lambda/2} \hat{G}\cdot(\phi_1\hat{\eta}_1 + \phi_2\hat{\eta}_2) \quad (12)$$

with the additional constraint that ϕ_1 and ϕ_2 remain finite when $w \to 0$.

The operators $L(d,\epsilon)$ and $\mathcal{L}(d,\alpha)$ reduce in the stripe $-1 \leqslant w \leqslant 1$ to the form

$$L = A_{ww}\partial_w^2 + A_{\chi\chi}\partial_{\chi^2} + A_{\chi^w}\partial_\chi\partial_w + A_\chi\partial_\chi + A_w\partial_w + A, \quad (13)$$

where the A's are 2×2 matrices. They were computed with the help of the symbolic software MAPLE and the explicit expressions in two dimensions are given in Appendix A.

The boundary conditions in the (χ,w) plane result from the various symmetries of the problem. When $w=0$ (the points are aligned, $\vec{\rho}_1$ and $\vec{\rho}_2$ are parallel to $\hat{\eta}_2$), the correlation function must depend on $\hat{\eta}_2$ only, implying that $\phi_1(\chi, w=0)=0$. Also, when the points are close to perfect alignment ($w \ll 1$), the function ϕ_2 is invariant under $w \to -w$, so $\partial_w\phi_2(\chi,w=0)=0$. The $\mathcal{S}_3$ symmetry already mentioned implies that the functions ϕ_1 and ϕ_2 are periodic in χ, with a period equal to $2\pi/3$. The $|w|=1$ (or, equivalently, $\xi_2 = |\xi_1|$) case corresponds to an isosceles triangle $|\vec{r}_1 - \vec{r}_2| = |\vec{r}_2 - \vec{r}_3| = |\vec{r}_3 - \vec{r}_1|$. In this case, the $\mathcal{S}_3$ permutation implies that the function Ψ is invariant when the vectors $\hat{\eta}_1$ and $\hat{\eta}_2$ are rotated by $2\pi/3$. As a result, $\phi_1(\chi, w=\pm 1) = -\frac{1}{2}\phi_1(\chi, w=\pm 1) \pm (\sqrt{3}/2)\phi_2(\chi, w=\pm 1)$ and $\phi_2(\chi, w=\pm 1) = -\frac{1}{2}\phi_2(\chi, w=\pm 1) \mp (\sqrt{3}/2)\phi_1(\chi, w=\pm 1)$, so $\phi_1(\chi, w=\pm 1) = \phi_2(\chi, w=\pm 1) = 0$.

Because the function is odd when $\vec{\rho}_{1,2} \to -\vec{\rho}_{1,2}$, $\phi_{1,2}(\chi+\pi, w) = -\phi_{1,2}(\chi, w)$. Finally, the function is invariant when $(\vec{r}_1, \vec{r}_2) \to (\vec{r}_2, \vec{r}_1)$, that is, when $\vec{\rho}_1 \to -\vec{\rho}_1$ and $\vec{\rho}_2 \to \vec{\rho}_2$, which amounts to $(\chi, w) \to (-\chi, -w)$. Combining these symmetries, one concludes that it is enough to restrict to the rectangle $0 \leqslant w \leqslant 1$, $0 \leqslant \chi \leqslant \pi/6$, with the boundary conditions

$$\phi_1(\chi, w=0) = \frac{\partial\phi_2}{\partial w}(\chi, w=0) = 0, \quad (14a)$$

$$\phi_1(\chi=0, w) = \frac{\partial\phi_2}{\partial w}(\chi=0, w) = 0, \quad (14b)$$

$$\phi_2(\chi=\pi/6, w) = \frac{\partial\phi_1}{\partial\chi}(\chi=\pi/6, w) = 0, \quad (14c)$$

and

$$\phi_1(\chi, w=1) = \phi_2(\chi, w=1) = 0. \quad (14d)$$

The problem thus reduces to an elliptic eigenvalue problem [22]. The scaling exponent λ appears as a nonlinear ''eigenvalue,'' which has to be found as a function of d and α or ϵ.

C. Properties of the Batchelor-Kraichnan operator

An important property is that the problem can be solved exactly when $\alpha = 0$ or $\epsilon = 0$. This is a consequence of the SL(2) symmetry of the problem [17,18]; see also Ref. [23] in the case of the four-point correlation function. Indeed, the Batchelor-Kraichnan operator expresses the condition of stationarity of the correlation function when the flow reduces to a random, large-scale strain, implying that the operator is invariant when $(\vec{\rho}_1, \vec{\rho}_2)$ is replaced by $A(\vec{\rho}_1, \vec{\rho}_2)$, where A is a real matrix of determinant 1. This can be formally checked by introducing the generators of the group SL(2): $G_{ij} = \rho_i^a \partial_{\rho_j^a} - \frac{1}{2}\Lambda$, where Λ is the dilation operator, already defined. The operator $G^2 = \frac{1}{2}\Sigma G_{ij}G_{ji}$ commutes with all the generators of the group [Casimir operators of SL(2)]. Also, the operators Λ, G^2, and L^2 commute with each other. It turns out that the Batchelor-Kraichnan operator $\mathcal{L}_0$ can be expressed as

$$\mathcal{L}_0(d) = -(d+1)L^2 + 2dG^2 + \frac{d-2}{4d}\Lambda(\Lambda+2d). \quad (15)$$

Interestingly, one may construct an explicit integral representation of the solutions. In two dimensions, one notes that the operators L^2, G^2, Λ, and $G_z = i(G_{12} - G_{21})$ commute with each other. The function

$$\psi^\lambda_{\nu,m,q} \equiv \zeta^{(\lambda/2)-\nu} \int_0^{2\pi} \frac{d\phi}{2\pi} \times \int_0^{2\pi} \frac{d\theta}{2\pi} e^{im\theta + q\phi}[\hat{n}_i(\phi)\rho_i^a \hat{e}_a(\theta)]^{2\nu} \quad (16a)$$

is an eigenstate of (L^2, G^2, G_z, Λ) with the quantum numbers $[1, \nu(\nu+1), q, \lambda]$. In Eq. (16a), $m = \pm 1$ and $\hat{n}(\psi)$ and $\hat{e}(\theta)$ are two unit vectors in two dimensions, in the direction given by the angles θ and ψ, respectively.

With the parametrization of the vectors $(\vec{\rho}_1, \vec{\rho}_2)$ and with the definition $\hat{\eta}_1 = (\cos(\gamma), \sin(\gamma))$ and $\hat{\eta}_2 = (-\sin(\gamma), \cos(\gamma))$, the function $\psi^\lambda_{\nu,m,q}$ reduces to

$$\psi^{\lambda}_{\nu,m,q}=(\xi_1\xi_2)^{(\lambda-\nu)/2}e^{i(q\chi+m\gamma)}\times\int_0^{2\pi}d\phi[\xi_1\cos(\phi)-i\xi_2\sin(\phi)]\times[\xi_1^2\cos(\phi)^2+\xi_2^2\sin(\phi)^2]^{\nu-1/2}. \quad (16b)$$

The spectrum of the operator $\mathcal{L}_0$ can be determined by using the boundary conditions (14) [17,21]. They lead to $\lambda=1$ and $\nu=1/2$, but leave an infinite degeneracy in q: $q=3(2p+1)$, where p is an integer.

The technical details are more involved in three dimensions (one needs six quantum numbers to completely specify the problem). A very similar integral representation of the eigenmodes of the Batchelor-Kraichnan operator can be found, with the same degeneracy in q and the same value of the scaling exponent $\lambda=1$.

D. Perturbation theory

The large degeneracy is lifted by the perturbation term when ϵ or $\alpha\neq 0$ [18,20,21]. A very important feature of the perturbation theory is that close to the line $w=0$ (i.e., when the three points are almost aligned), the operator $\mathcal{L}_0$ is formally much smaller than the perturbation operator. Near $w=0$, $\mathcal{L}_0$ in three dimensions reduces to

$$\frac{1}{2d}\mathcal{L}_0\begin{pmatrix}\phi_1\\ \phi_2\end{pmatrix}=\left[w^2\partial_{w^2}-2\lambda w\partial_w+w^2\partial_{\chi^2}+2w\begin{pmatrix}0 & -1\\ 1 & 0\end{pmatrix}\right]\times\begin{pmatrix}\phi_1\\ \phi_2\end{pmatrix}, \quad (17a)$$

whereas $\mathcal{L}_D$ reduces to

$$\frac{1}{2d}\mathcal{L}_D\begin{pmatrix}\phi_1\\ \phi_2\end{pmatrix}=\tilde{\beta}(\chi)\left[\partial_w^2+\frac{2}{w}\partial_w+\partial_{\chi^2}+2w\begin{pmatrix}0 & -1\\ 1 & 0\end{pmatrix}\right]\begin{pmatrix}\phi_1\\ \phi_2\end{pmatrix}+\tilde{\beta}(\chi)\begin{pmatrix}-4\phi_1/w^2\\ (-1+\lambda^2+4\lambda)\phi_2\end{pmatrix}, \quad (17b)$$

where $\tilde{\beta}(\chi)=([1-\cos(2\chi)]\{1-\cos[2(\chi+2\pi/3)]\}\{1-\cos[2(\chi-2\pi/3)]\})^{2/3}$. A comparison Eqs. (17a) and (17b) shows that the perturbation term is formally dominant for $|w|\ll\alpha^{1/2}$. Similar considerations lead to the conclusion that, for $-\ln|w|\ll\epsilon^{-1}$, the Batchelor operator is small compared to the perturbation term. Because of this property, one needs to use matched asymptotic expansions. Technically, in the case of the K model in three dimensions, one defines a scaled variable $z=w/\sqrt{\alpha}$ and one expands the differential operator in powers of $\alpha^{1/2}$. Away from the points $\chi=0,\pm 2\pi/3$, the dependence on χ is slow ($\partial_\chi\ll\partial_w$). The problem therefore reduces to a single differential equation on z, which can be solved with the condition $\phi_2(\chi,w=0)=a(\chi)$. Imposing that for $z\to\infty$ but $w\to 0$ (in the matching region) the solution consists of a superposition of q modes, one obtains that the function $a(\chi)$ must satisfy the ordinary differential equation

$$\tilde{\beta}(\chi)(a''+a)+\frac{20}{9}\delta a=0, \quad (18)$$

with $\delta\equiv\lim_{\alpha\to 0}(\lambda-1)/\alpha$ (for the K model in three dimensions). The boundary conditions impose that $a(\chi=\pi/6)=0$. Near $\chi=0$, the solution of Eq. (18) behaves as

$$a(\chi)=a_0|\chi|^{2/3}(1+|\chi|^{2/3}+\cdots)+a_1|\chi|(1+|\chi|^{2/3}+\cdots). \quad (19a)$$

As there exists a unique solution of Eq. (18) with $a(\pi/6)=0$ and $a'(\pi/6)=-2$, say, the coefficients a_0 and a_1 are completely determined by δ. To actually obtain a solution of the problem, one has to make sure that the solution away from $\chi=0$ matches with the solution of the full problem. This is a nontrivial task, as one has to solve a fully two-dimensional elliptic problem in the neighborhood of the point $(\chi,w)=(0,0)$, with unspecified boundary conditions. A local expansion, valid in a region of size $\sim\alpha^{3/2}$, can be relatively easily generated (see Appendix B). However, this expansion does *not* help to match the solution further away (for $\chi\ll 1$), as there is no overlap between the two asymptotic domains.

For the white-noise problem, the function $a(\chi)$ satisfies the ordinary differential equation (18), with $f(\chi)=[\cos^2(\chi)-1][4\cos^2(\chi)-1]\ln[1-\cos(2\chi)]+\cdots$, where the ellipsis denotes the terms obtained by replacing χ by $\chi\pm 2\pi/3$ in the previous expression. The behavior near $\chi=0$ is therefore given by

$$a(\chi)=a_0|\ln(\chi)|^{-\delta}(1+\cdots)+a_1|\chi|(1+\cdots). \quad (19b)$$

The inner problem, close to $(\chi,w)=(0,0)$, has been analyzed, leading to the conclusion that the solution is $\delta=0$ [20], a prediction confirmed by the numerical results [22].

E. Integral representation of the correlation function

The solutions of the K model and of the white-noise problem near the Batchelor limit can be parametrized by an integral representation, valid away from collinearity ($w=0$). Namely, for $w\gg\alpha^{1/2}$, the operator $\mathcal{L}(d,\alpha)$ reduces to the Batchelor-Kraichnan operator, up to a small correction, so its solution is a combination of zero modes of this operator. Summing the modes $\psi^{\lambda}_{\nu,m,q}$ [see Eq. (16a)], one obtains the representation

$$\Psi=\hat{G}\cdot\int_0^{2\pi}\frac{\xi_1\cos(\phi)\hat{\eta}_1+\xi_2\sin(\phi)\hat{\eta}_2}{[\xi_1^2\cos(\phi)^2+\xi_2^2\sin(\phi)^2]^{(1-\lambda)/2}}f(\chi+\phi)d\phi. \quad (20)$$

Imposing that this function tends to $a(\chi)$ when $w\to 0$ allows one to relate $f(\chi)$ to $a(\chi)$. When $|\xi_1|\ll\xi_2$ and in the limit $\lambda\approx 1$, one finds that $a(\chi)=\int_0^{2\pi}\sin(\phi)|\sin(\phi)|^{\lambda-1}f(\phi+\chi)d\phi$. The function $a(\chi)$ is even and is expected to be represented by a sum of singularities of the form $|\chi|^{\mu}$ singularity [the two dominant exponents are $\mu=2/3$ and 1; see Eq. (19a)]. The function $f(\chi)$ is therefore odd and has singularities of the form $f(\chi)\sim\chi|\chi|^{\mu-2-\lambda}$ when $\chi\to 0$. This suggests to

approximate the three-point correlation function by Eq. (20), with a function f that contains the two dominant singularities compatible with Eq. (19):

$$f(\chi)=1+(f_{2/3}+f_1|\chi|^{1/3})/|\chi|^{1/3+\lambda}+(f_{2/3}+f_1|\pi/3-\chi|^{1/3})/|\pi/3-\chi|^{1/3+\lambda} \quad \text{for } 0\leqslant\chi\leqslant\pi/3, \quad (21)$$

where $f_{2/3}$ and f_1 are two parameters. This parametrization is expected to work for small values of α and away from $w=0$.

An important consequence of the integral representation (20) is that it suggests that the overall shape of the three-point correlation function depends mostly on the global scaling exponent λ and the exponent of the singularity describing the limit where two points merge.

In the white-noise problem and for finite values of ϵ, the fact that $\delta=0$ [20,22] implies that the dominant singularity of f is $f(\chi)\approx\chi/|\chi|^2$, so that away from $w=0$ and for small values of ϵ, the integral representation (20) with $f_{2/3}=0$ should provide a good parametrization of the solution. At larger values of ϵ, the solution near $\rho_1=0$ can be expanded in powers of $|\rho_1|^\epsilon$. This suggests that $a(\chi)$ will have singularities of the form $|\chi|^{n\epsilon}$, and for not too small values of ϵ, one may also try to compare the solution with the integral representation with the appropriate singularities. In particular, for $\epsilon=2/3$, one may expect that the representation used for the K model will also represent the solution qualitatively.

III. NUMERICAL METHODS

The strategy to determine the zero modes of the operator consists in discretizing the operators $L(d,\epsilon)$ or $\mathcal{L}(d,\alpha)$, which therefore become matrices, and to compute numerically their determinant as a function of λ, the scaling exponent.

We have chosen here to use centered finite differences. We work with a rectangular, separable mesh. The solution is stored as a sequence of consecutive lines $w=$const, so the differential operator is reduced to a banded matrix. The determinant can be found by LU decomposition, a standard method [26], using public domain routines. If N discretization points in each direction are used, then both the amount of memory space and CPU time needed are of order $\sim N^3$. Our calculation were performed on a workstation ($N\lesssim 70$) and on a Cray Supercomputer C98 ($N\lesssim 160$).

The differential operators $L(d,\epsilon)$ and $\mathcal{L}(d,\alpha)$ are singular near $w=0$ and $\chi=0$, as some of the coefficients go to zero. For this reason, the points $w=0$ and $\chi=0$ were not explicitly included in the calculation. Also, near $w=1$, the coefficient of ∂_w^2 diverges, leading to a $\sqrt{1-w^2}$ behavior of the solution near $w=1$. To make the solution smooth near $w=1$, we redefined a variable u by $1-u=\sqrt{1-w}$. The unfortunate feature of this change of variable is that it tends to refine the solution in the region near $w=1$ instead of the region near $w=0$, where they are much needed.

In order to properly resolve the solution in the singular region $|\rho_1|\to 0$ as well as in the vicinity of $w=0$, we implemented nonuniform meshes in both the χ and w directions. This was achieved by taking (in the w direction, for example) a function of the form $g_w(\theta)=u_w\theta+(1-u_w)\theta^2$, which maps (0,1) onto itself ($0\leqslant u_w\leqslant 1$). As u_w gets smaller, more points get pushed in the $w=0$ region, leading to an enhanced resolution in this area.

We checked thoroughly the calculation of the matrix by applying the discretized differential operator to a number of known functions. Examples include the q modes [see Eq. (16)], which are zero modes of the Batchelor operator when $\lambda=1$. They can be explicitly computed and expressed with elementary functions. We checked that when the number of points in each direction increases, both the maximum and the L_2 norm of $\|L(d,\epsilon=0)\binom{\phi_1}{\phi_2}\|$ decrease to zero.

The Laplacian term was checked by applying it to the ''coordinate functions''

$$\vec{\rho}_1=\begin{pmatrix}\xi_1\ \sin(\chi)\\ \xi_2\ \cos(\chi)\end{pmatrix},\quad \vec{\rho}_2=\begin{pmatrix}\xi_1\ \cos(\chi)\\ -\xi_2\ \sin(\chi)\end{pmatrix}$$

and making sure that when $\lambda=1$, $\nabla^2\vec{\rho}_1=\nabla^2\vec{\rho}_2=0$ (except near the boundaries). In the same spirit, we also checked that $(\rho_1^2+\rho_2^2)\nabla^2[(\rho_1^2+\rho_2^2)\vec{\rho}_{1,2}]=4(d+1)[(\rho_1^2+\rho_2^2)\vec{\rho}_{1,2}]$ (when $\lambda=3$).

To check the operator $L(d,\epsilon)$ (white-noise problem), we returned to the definition (4b) and checked individually each term in the sum. The polynomials $(\vec{\rho}_1)^2\vec{\rho}_1$ and $(\vec{\rho}_2)^2\vec{\rho}_1$ are eigenvectors of $(d+1-\epsilon)\vec{\rho}_1^2(\partial_1^a\partial_1^a-\frac{1}{3}\partial_2^a\partial_2^a)-(2-\epsilon)\rho_1^a\rho_1^b(\partial_1^a\partial_1^b-\frac{1}{3}\partial_2^a\partial_2^b)$ with the eigenvalues $2(d-1)(d+4-\epsilon)$ and $2(d-1)(d+2-\epsilon)$ ($\lambda=3$). This relation was checked directly on the discretized version of the differential operator. We also checked that the polynomial $P(\vec{\rho}_1,\vec{\rho}_2)\equiv(\rho_1^2-\rho_2^2)\vec{\rho}_2+2(\vec{\rho}_1\cdot\vec{\rho}_2)\vec{\rho}_1$ is a zero mode of $L(d,\epsilon=2)$ ($\lambda=3$).

In order to compute the eigenvalue, λ, we proceed by dichotomy, a straightforward operation once two values of λ are known, such that the determinants of the matrix are of opposite signs. A crude search was made at low resolution, which then provides a good starting point at higher resolution where the calculations are more expensive. The accuracy of the computed eigenvalue was set to better than five significant figures, which was reached in less than 15 iterations.

The ultimate test that convinced that our algorithm is properly working was obtained by studying the L model [obtained by replacing $(r_{12}^2r_{23}^2r_{31}^2)$ by R^6 in Eq. (5)]. The eigenfunctions are of the form $\phi_1=f_1^q(w)\cos(q\chi)$ and $\phi_2=f_2^q(w)\sin(q\chi)$. The functions $f_{1,2}^q(w)$ satisfy some ordinary differential equations, which define a boundary-value problem, and can be solved by the shooting method. The eigenvalues obtained from the full partial differential equation agree with the eigenvalues obtained by solving the system of differential equations and the agreement gets better when the mesh is refined (N increases).

IV. NUMERICAL RESULTS

A. Scaling exponents in the white-noise problem

The lowest branch of eigenvalues, computed as explained in the preceding section, are shown in Fig. 1 for the white-noise problem in 2 [Fig. 1(a)] and three-dimensions [Fig. 1(b)]. The convergence of our numerical results is very good

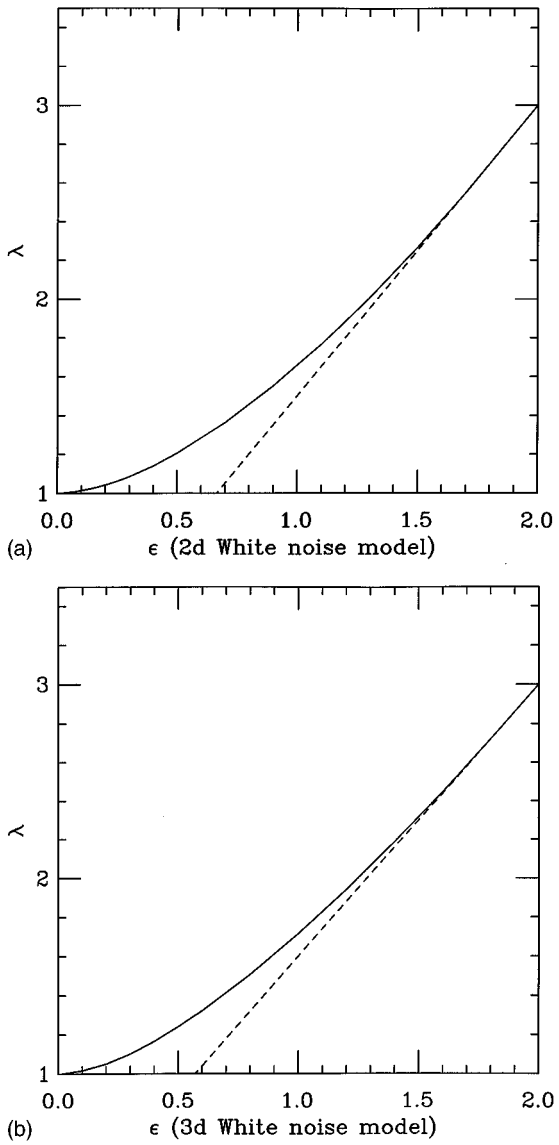

FIG. 1. Scaling exponent of the three-point correlation function in (a) two and (b) three space dimensions for the white-noise model. The results were obtained with 160 grid points in each direction. The dashed lines correspond to the perturbative result $\lambda=3-(d+4)/(d+2)(2-\epsilon)$ near $\epsilon=2$. The exponents are less than $1+\epsilon$, implying anomalous scaling in this model.

near $\epsilon=2$: The results obtained with $N=40$ and 160 evenly spaced mesh points agree with four significant figures. In this range of parameters, the perturbation analysis in $2-\epsilon$ predicts that [22,24,25]

$$\lambda(\epsilon)=3-\left(\frac{d+2}{d+4}\right)(2-\epsilon). \tag{22}$$

This prediction works extremely well, as shown in Fig. 1, where the straight lines corresponding to Eq. (22) are plotted.

The convergence near $\epsilon=0$ is a more delicate matter due to the very singular nature of the limit. Figure 2 shows the values of $\lambda^N(\epsilon)$ of the calculated exponent for a set of values of the number N of grid points (these values were obtained with refined meshes, with $u_\chi=0.3$ and $u_w=0.1$). As the

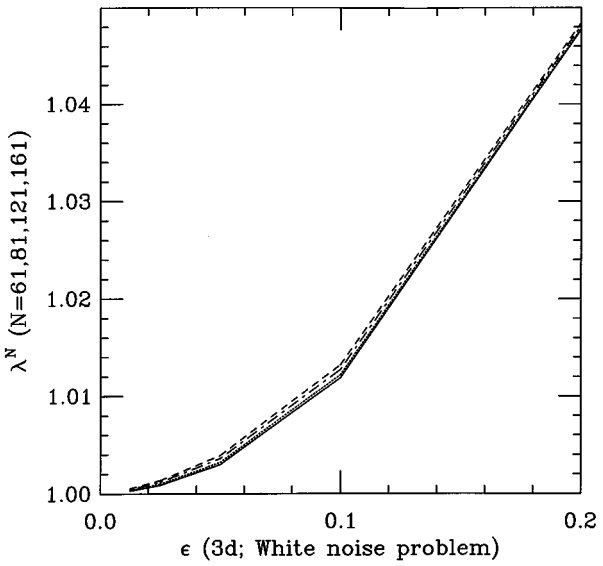

FIG. 2. Convergence of the numerical results near $\epsilon=0$ of the exponent in the white-noise model ($3d$) when the number of grid points increases. The full line is the result of the extrapolation $N\to\infty$ using Eq. (23). We used a refined mesh near $\chi=0$, $w=0$: $u_\chi=0.3$, $u_w=0.1$.

number of grid points N increases, the value of $\lambda^N(\epsilon)$ decreases. The full line was obtained by fitting the eigenvalues by

$$\lambda'^N(\epsilon)=\lambda^\infty(\epsilon)+\Delta\lambda(\epsilon)/N. \tag{23}$$

The quality of the fit, measured by $|[\lambda^N(\epsilon)-\lambda'^N(\epsilon)]/[\lambda^N(\epsilon)-1]|$ was found to be better than 10^{-2} for all the values of N considered, down to $\epsilon=0.031\,25$. Our results give clear evidence that the slope of the curve $[\lambda(\epsilon)-1]/\epsilon$ goes to 0 when $\epsilon\to0$. This generally agrees with the prediction of perturbation theory $\lambda\approx1+\delta\epsilon$, with $\delta=0$.

We emphasize that the branch we found implies an anomalous scaling of the three-point correlation function for any value of ϵ. Indeed, the naive scaling exponent resulting from dimensional analysis of the differential equation is $\lambda=1+\epsilon$. The exponents determined here is smaller than $1+\epsilon$, establishing the existence of anomalous scaling in this model.

The branch of solutions we have described seems to be the lowest branch of a presumably infinite sequence of solutions. The next branch of solutions starts from $\lambda=5$ near $\epsilon=2$ $[\lambda=5-\frac{6}{5}(2-\epsilon)]$ in three dimensions and goes down towards $\lambda=1$ near $\epsilon=0$; see Fig. 3. In view of the convergence problem of our numerical algorithm near $\epsilon=0$, it is difficult to determine precisely the behavior near $\epsilon=0$.

B. Scaling exponent in the *K* model

The result for the lowest branch of solutions of the K model are shown in Fig. 4, in two [Fig. 4(a)] and three dimensions [Fig. 4(b)]. The convergence problem alluded to in the preceding subsection are also present in this problem. In fact, the problem appears much more severe in two dimensions, where a strong refinement of the mesh near (0,0) was

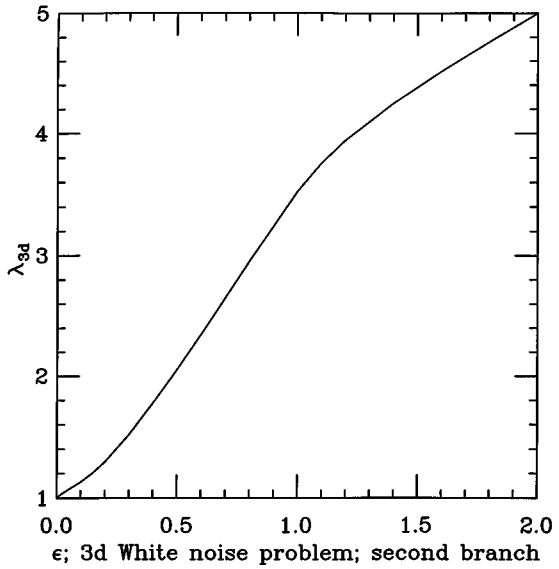

FIG. 3. Scaling exponent for the higher branch of solutions for the white-noise problem in three dimensions.

needed in order to obtain sensible results (we had to take $u_\chi = 0.1$ and $u_w = 0.05$). In comparison, the results in three dimensions converged much better. Another unexpected difficulty has to do with the small size of the asymptotic region. Figure 5 shows the value of $\delta(\alpha) \equiv [\lambda(\alpha) - 1]/\alpha$, after extrapolating the values of the exponents determined for a sequence of values of N with a fit of the form (23). The dashed line shows a fit of $\delta(\alpha)$ in three dimensions by a function of the form $\delta(\alpha) \approx a_1 \alpha^{1/2} + a_2 \alpha + a_3 \alpha^{3/2}$, with $a_1 \approx 2$, $a_2 \approx -2.5$, and $a_3 \approx 1$.

In addition to the lowest ''fundamental'' branch of solutions, there exists a seemingly infinite number of higher branches. We have investigated the two next higher branches of solutions, shown in Fig. 6. The numerics suggests that the behavior of λ is of the form $\lambda = 1 + \delta_{2,3}\alpha + O(\alpha^{3/2})$, with $\delta_2 \approx 4.5$ and $\delta_3 \approx 12$.

The results regarding the lowest branch of solution (Fig. 4) agree with the predictions of the perturbation analysis [21]. The numerical results presented here is also consistent with the perturbative calculation in the sense that the function $a(\chi)$ determined numerically seems to converge towards the solution of Eq. (18) with $\delta = 0$, which reduces simply to $a(\chi) = 2\sin(\pi/6 - \chi)$ (see Fig. 7). This shows that the leading singularity near $\chi = 0$ is $a(\chi) \approx |\chi|$, as it was the case in the white-noise problem near $\epsilon = 0$.

Because our numerics is not precise enough to capture accurately the higher branches of solution near $\chi = 0$, it is difficult to make detailed comparisons between the predictions of Eq. (18) and the function $\phi_2(\chi, w = 0)$ determined numerically. Still, the solutions corresponding to higher-order branches have an increasing number of nodes, as predicted from Eq. (18), which is of Sturm-Liouville type.

C. Structure of the correlation function when two points merge

As already explained, the structure of the wave function near $(\chi, w) = (0,0)$, that is, when two points merge, is a very important aspect of the solution. We discuss here our numerical results in this limit.

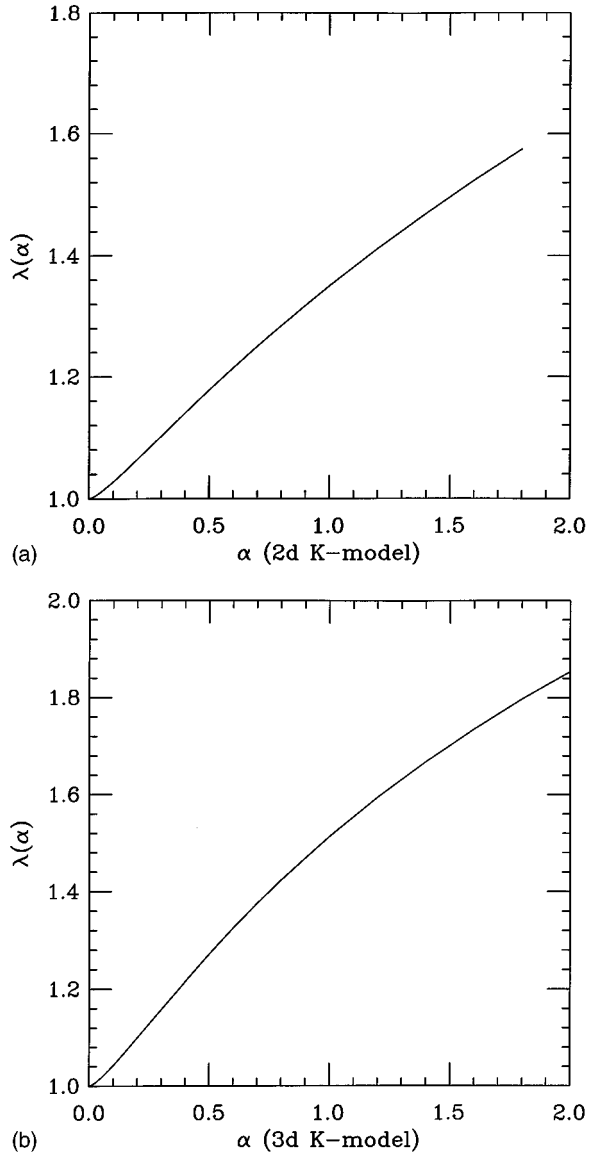

FIG. 4. Scaling exponent of the three-point correlation function in (a) two and (b) three space dimensions for the K model. The results were obtained with 160 grid points in each direction, with a refined mesh near $(\chi, w) = (0,0)$ ($u_\chi = 0.1$, $u_w = 0.05$ in two dimensions and $u_\chi = 0.3$, $u_w = 0.1$ in three dimensions).

In order to compare with the expansion near $|\rho_1| = 0$ in the innermost region (see Appendix B) we have investigated the three-point correlation function at a fixed value of $\vec{\rho}_2$ $(= \hat{y})$ and as a function of $\vec{\rho}_1$. At a fixed value of the norm of $\vec{\rho}_1$ (denoted ρ), the wave function depends only on the angle $\theta = \arctan(w/2\chi)$ and a straightforward decomposition in Fourier series $\Sigma_m A_m(\rho)\cos(m\theta)$ allows one to extract the various waves, to be compared with Eqs. (B3) and (B4).

Figure 8 shows the ρ dependence of the modes $m = 0$ (s wave) and $m = 2$ for $\alpha = 0.006\,25$, 0.025, 0.1, and 0.4. The ρ dependence at the two largest values of α are consistent with the predictions of Appendix B: The $m = 0$ mode behaves as $-1 + \rho^{2/3}$, whereas the $m = 2$ mode behaves as $\rho^{4/3}$. For the smallest values of α ($\alpha = 0.006\,25$ and 0.025), the two components seem to behave linearly all the way down to very small values of ρ.

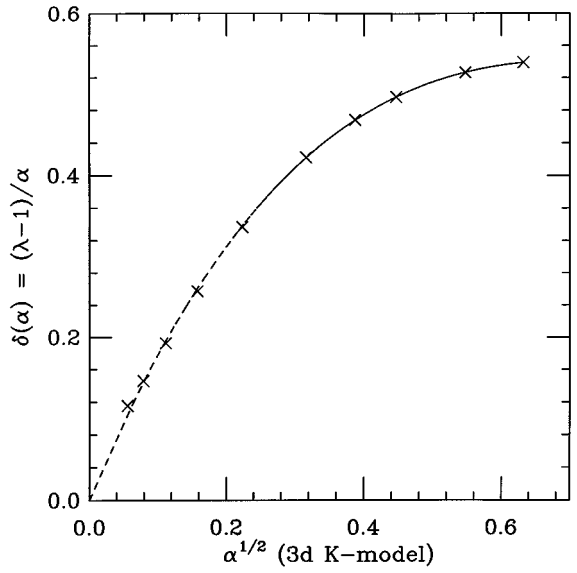

FIG. 5. Local slope $\delta(\alpha)\equiv[\lambda(\alpha)-1]/\alpha$ near $\alpha=0$ for the K model. The dashed line corresponds to a fit by a functional form $\delta(\alpha)\approx 2\alpha^{1/2}-2.5\alpha+\alpha^{3/2}$.

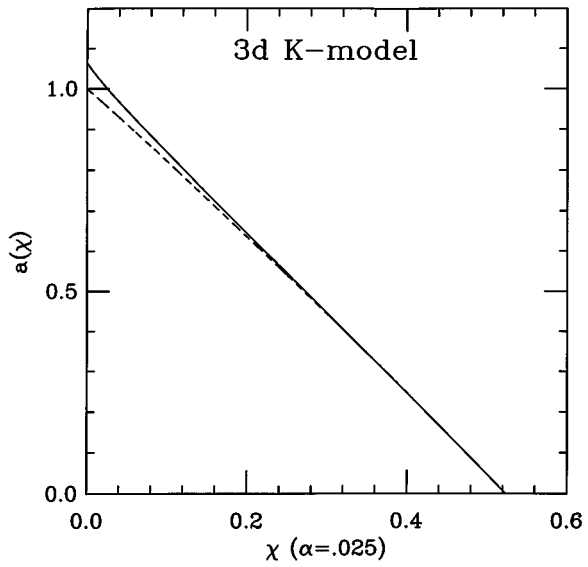

FIG. 7. Function $a(\chi)\equiv\phi_2(\chi,w=0)$ in three dimensions, determined numerically for $\alpha=0.025$ in the K model in three dimensions. The normalization is chosen so that $a'(\chi=\pi/6)=-2$. The function is very close to $2\sin(\pi/6-\chi)$, which is the solution of Eq. (18) with $\delta=0$; the agreement improves when α diminishes.

Our results are completely consistent with the numerical results concerning the dependence of λ as a function of α and with the expansion of the solution near $\rho=0$, described in Appendix B. Near $\alpha=0$, $(\lambda-1)/\alpha\to 0$, so the expansion in powers of $\rho^{2/3}$ presented in Appendix B is multiplied by an overall factor that goes to zero when $\alpha\to 0$. On top of it, the expansion is formally valid only in a very small neighborhood of $(\chi,w)=(0,0)$. This explains why the $\rho^{2/3}$ behavior cannot be seen for small values of α ($\alpha=0.006\,25$ and 0.025). For the larger values of α, the dependence near $\rho=0$ is consistent with the predictions of Appendix B. In particular, the leading-order coefficients of the s and d waves in the $\rho^{2/3}$ expansion of Appendix B agree with the results shown in Fig. 8. The linear dependence on ρ of the $m=0$ and 2 wave can be understood with the help of the integral representation (19) and (20), as we now discuss.

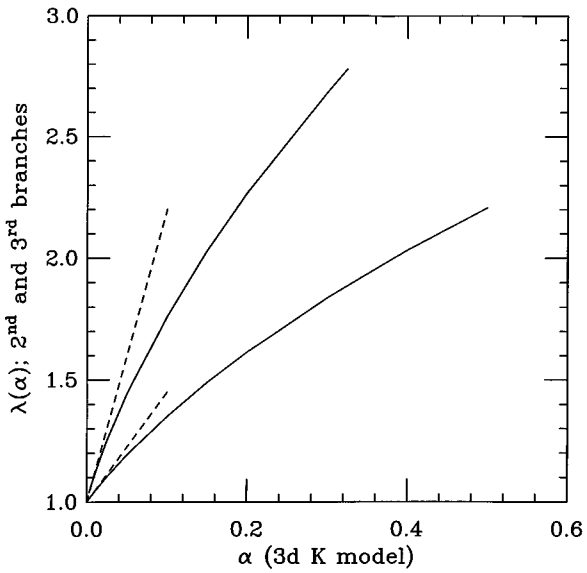

FIG. 6. Scaling exponent for the next two higher branches of solutions of the K model in three dimensions. Near $\alpha=0$, $\lambda_2(\alpha)\approx 1+4.5\alpha$ and $\lambda_3(\alpha)\approx 1+12\alpha$.

D. Structure of the correlation function when $\alpha\to 0$

We restrict the discussion here to the K model, although many of the results presented apply as well to the white-noise problem. The results of Sec. IV B imply that the dominant singularity of $a(\chi)$ is $\sim|\chi|$, so the coefficient $f_{2/3}$ in Eq. (19) must be zero. The calculation of the integral representation turned out to be fairly insensitive to the precise value of f_1, provided it is not too small. We have chosen here $f_1=10$.

Figure 9 shows the isocontour patterns of the components ϕ_1 and ϕ_2 in the rectangle $(0,\pi/6)\times(0,1)$ in the (χ,w) plane, obtained numerically for $\alpha=0.006\,25$. The tick marks along the perimeters in Fig. 9 show the mesh points used in the calculation. The isocontour lines obtained from the integral representation (20) and (21) with $\lambda=1.000\,92$, $f_{2/3}=0$, and $f_1=10$ are very close to Fig. 9. A more quantitative comparison can be obtained by computing the difference between the numerical solution and the integral representation. Figure 10 shows the isocontour lines of this difference. As expected, the difference is largest near the line $w=0$. To be more precise, one may compute the L_2 norm of the difference between two solutions ϕ and ψ as the minimum of $\|\phi-c\psi\|$ on c. The L_2 norm of the difference for $\alpha=0.006\,25$ is less than 2% of the L_2 norm of the solution. The difference between the solution and the integral representation (20) and (21) computed from Eqs. (20) and (21) ($f_{2/3}=0$, $f_1=10$) is shown in Fig. 11 as a function of α. The difference goes to zero when $\alpha\to 0$ like $\alpha^{2/3}$.

The structure of the integral representation near the point $(\chi,w)=(0,0)$ can be determined analytically:

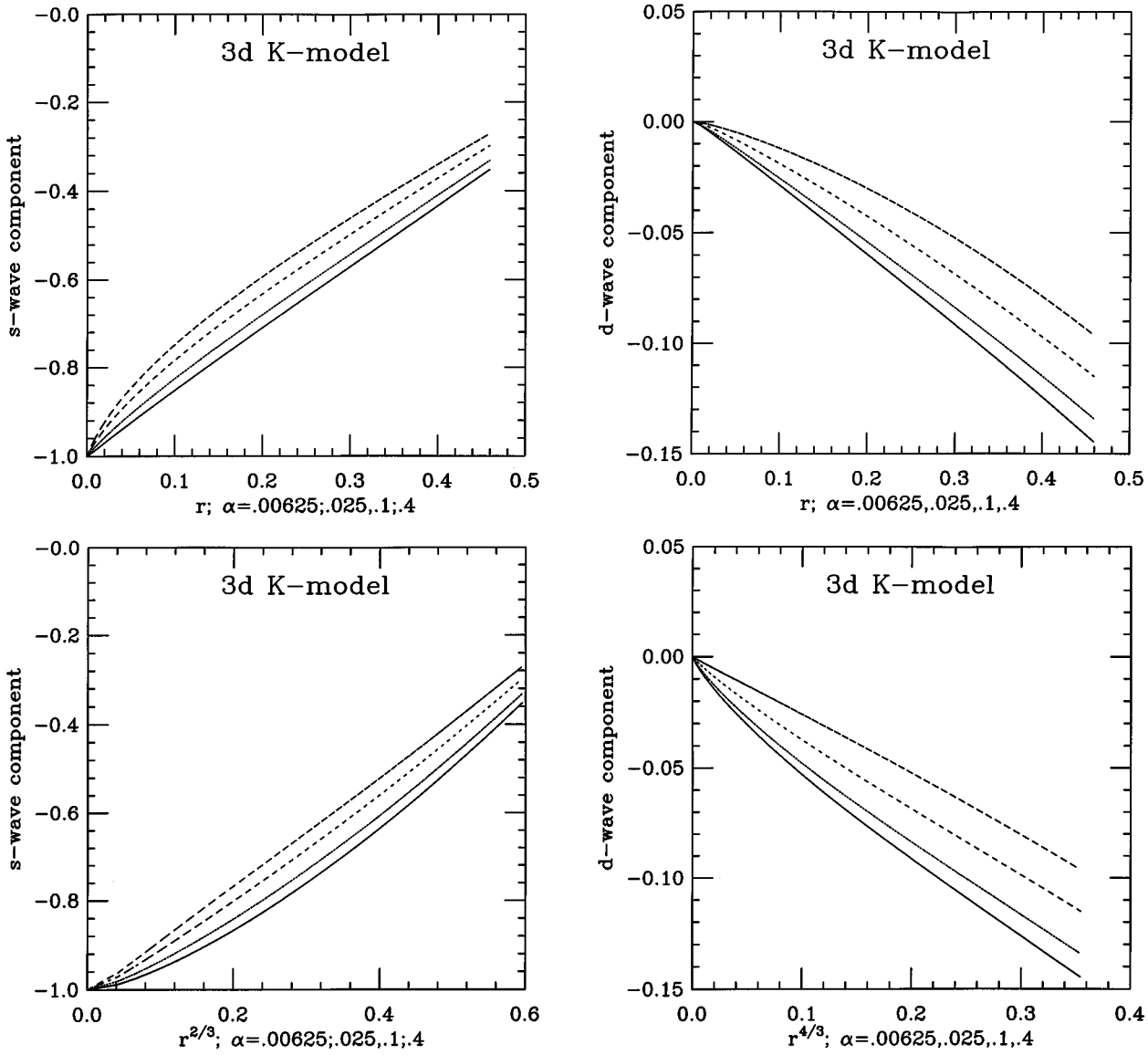

FIG. 8. The s-wave component of the solution of the K model in three dimensions as a function of (a) ρ and (b) $\rho^{2/3}$ and the d-wave component of the solution as a function of (c) ρ and (d) $\rho^{4/3}$. The values of α are 0.006 25, 0.025, 0.1, and 0.4. At the largest value of α, the s wave behaves as $-1+\text{const}\times\rho^{2/3}$ and the d wave as $\rho^{4/3}$.

$$\phi_1 = w(\theta - \pi/2), \quad \phi_2 = \text{const} + 2\chi(\theta - \pi/2), \qquad (24)$$

with $\theta = \arctan(w/2\chi)$ (see Appendix C). It implies that both the $m=0$ and 2 modes behave linearly with $|\rho|$, as found numerically. We emphasize that the very good agreement found with the integral representation crucially depends on the fact that the $|\chi|^{2/3}$ singularity is not present in the integral representation [$f_{2/3}=0$ in Eq. (21)].

Our results show that very near $\alpha=0$, the wave function can be precisely fit by the integral representation (20) and (21). It is remarkable that the solution of this nontrivial problem can be expressed by a simple integral, involving only elementary functions.

Very similar results can be obtained for the white-noise problem since it was also found in this limit that the dominant singularity of the function $a(\chi)$ is $\sim|\chi|$. We merely show here the difference between the numerical solution and the integral representation (Fig. 12). As in the K model, the difference between the two solutions goes to zero when $\epsilon \to 0$.

E. Structure of the correlation function for larger values of α

Figure 13 (Fig. 14) shows the isocontour lines in the (χ, w) plane of the function (ϕ_1, ϕ_2) for the K model for the value $\alpha=0.7$ (for the white-noise problem for $\epsilon=2/3$). In the latter case, the correlation function is expected to behave as $|\vec{r}_1-\vec{r}_2|^{2/3}$ when $|\vec{r}_1-\vec{r}_2| \ll |\vec{r}_1-\vec{r}_3| \sim |\vec{r}_2-\vec{r}_3|$, like in the K model. The scaling exponents are $\lambda(\alpha=0.7)=1.375$ and $\lambda(\epsilon=2/3)=1.381$, so the two solutions have very close overall scaling exponents, as well as the same limit when two points get close.

Figures 13 and 14 show that the overall structures of the functions are very similar. The difference between the solutions corresponding to $\epsilon=2/3$ and $\alpha=0.7$ ($\alpha=0.1$) is found

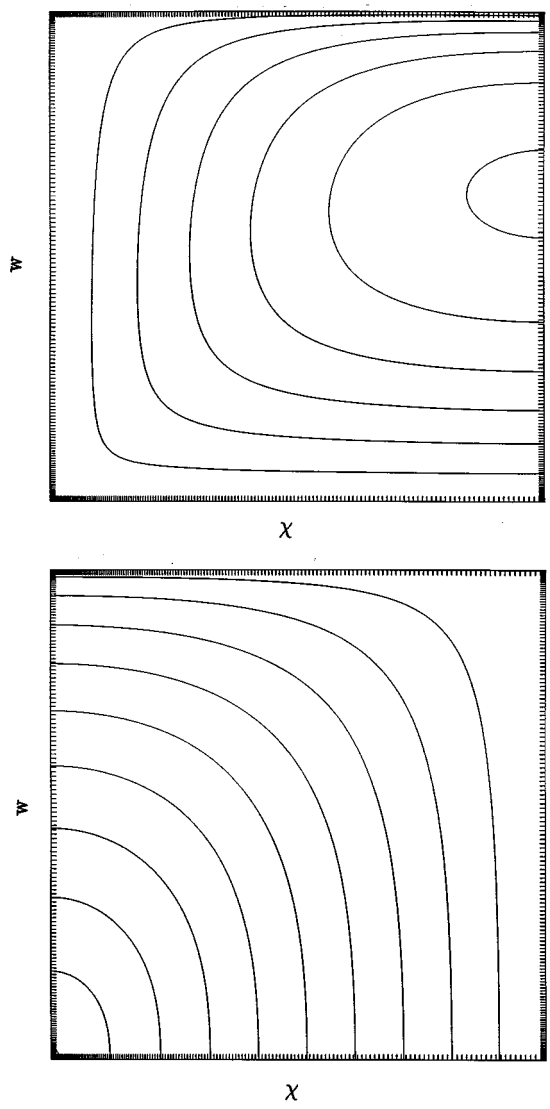

FIG. 9. Isocontour line pattern in the (χ,w) plane of the function (a) ϕ_1 and (b) ϕ_2 determined numerically for the K model in three dimensions for $\alpha=0.006\,25$. The tick marks show the grid points. The exponent is $\lambda=1.000\,91$. The contour intervals are 5×10^{-2} (a) and 10^{-1} (b).

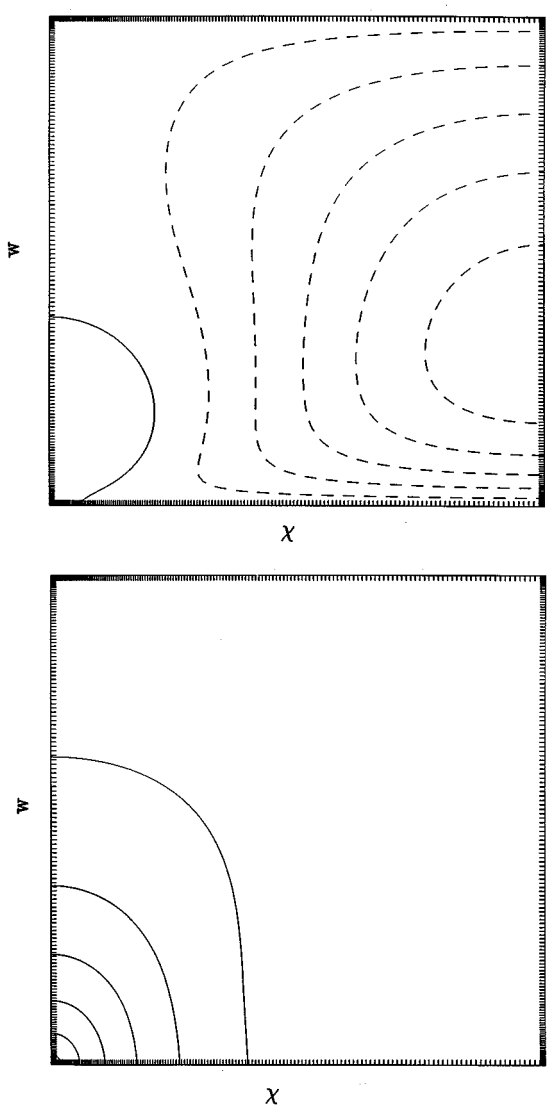

FIG. 10. Differences between the numerical solutions obtained for $\alpha=0.006\,25$ (Fig. 8) and the integral representation. The L_2 norm of the difference is $\approx1.5\%$ of the norm of the numerical solution. The countour intervals are 2×10^{-3} (a) amd 8×10^{-3} (b).

to be $\sim3\%$ ($\sim13\%$) of the norm of either wave function. This similarity may be understood to some extent as resulting from the parametrization (20) of the solution, which depends essentially on the overall exponent of the solution λ and the exponent of the singularity of the wave function near $|\rho_1|=0$. From this point of view, since the solutions corresponding to $\alpha=0.7$ and $\epsilon=2/3$ have very close scaling exponents $\lambda=1.375$ and 1.381 and the same power law when two points get very close, the integral representation (20) predicts that the two wave functions are very close in the regions where Eq. (20) is valid (away from $w\sim0$).

As the values of the parameters α and ϵ compared here are not so small, one has to take the integral representation with some care. Higher-order terms in the perturbation expansion presumably become large and may introduce significant corrections away from the $w=0$ axis. For this reason, the integral representation is not expected to give a very precise representation of the solution. Still, it is remarkable that the two solutions are so close.

F. Test of the SL(2) symmetry

The existence of the SL(2) symmetry of the Batchelor Kraichnan operator has very important consequences in this problem. An interesting question is how much of the symmetry remains when the perturbation is turned on. The goal here is to understand whether the SL(2) symmetry could be observed in experiments.

In order to test the SL(2) symmetry in this problem, we simply apply the G^2 operator to the wave function determined numerically. It the symmetry holds, the eigenfunction should remain an eigenvalue of G^2. In the following, we study how close the solution remains to an eigenvalue of G^2 so as to understand whether the SL(2) symmetry holds.

Technically, the operator G^2 can be simply written by separating the $m=\pm1$, $q=\pm(6p+3)p\geqslant0$ components, where m is the azimuthal quantum number and q is the quantum number associated with G_z in two dimensions; see Sec. II D. This leads us to expand the numerical wave function

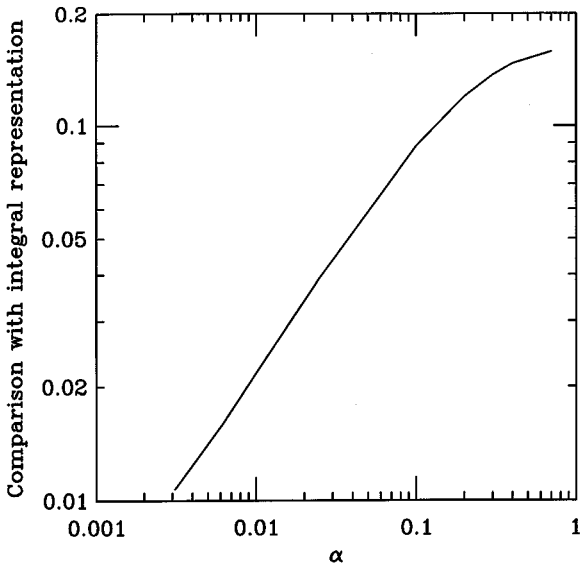

FIG. 11. The L_2 norm of the difference of the solution of the K model and of the integral representation, obtained with $f_{2/3}=0$, $f_1=10$, and λ determined numerically. The difference goes to zero like $\alpha^{2/3}$.

$\phi=\phi_1(\chi,w)\cos\theta+\phi_2(\chi,w)\sin\theta$ as a Fourier series in χ and θ:

$$\phi\equiv\sum_q \phi_1^q\cos(\theta)\sin(q\chi)+\phi_2^q\sin(\theta)\cos(q\chi). \quad (25)$$

By rearranging the terms in this series, one concludes that the functions $a_q^+(w)=[\phi_1^q(w)+\phi_2^q(w)]$ and $a_q^-(w)=[\phi_1^q(w)-\phi_2^q(w)]$ are the $(m=1,q)$ and $(m=-1,q)$ components of the solution. The operator G^2, acting on the function ϕ transforms $(a_q(w),b_q(w))$ into $(\tilde{a}_q^{\,+}(w),\tilde{a}_q^{\,-}(w))$, defined by

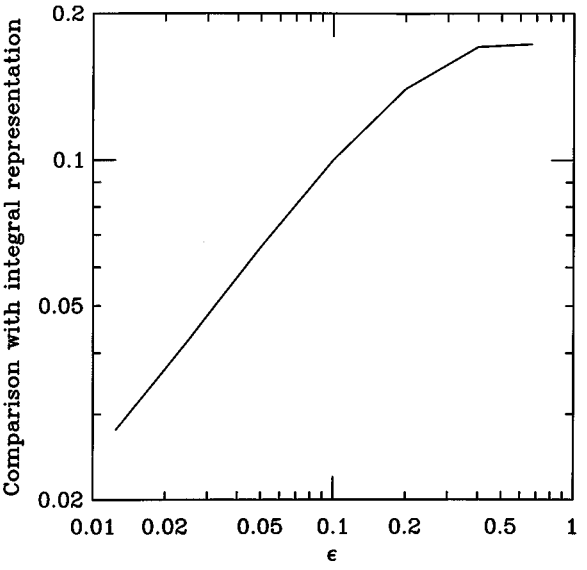

FIG. 12. The L_2 norm of the difference of the solution of the white-noise problem in three dimensions and of the integral representation, obtained with $f_{2/3}=0$, $f_1=10$, and λ determined numerically. The difference goes to zero like ϵ^x, $x\approx 0.6$.

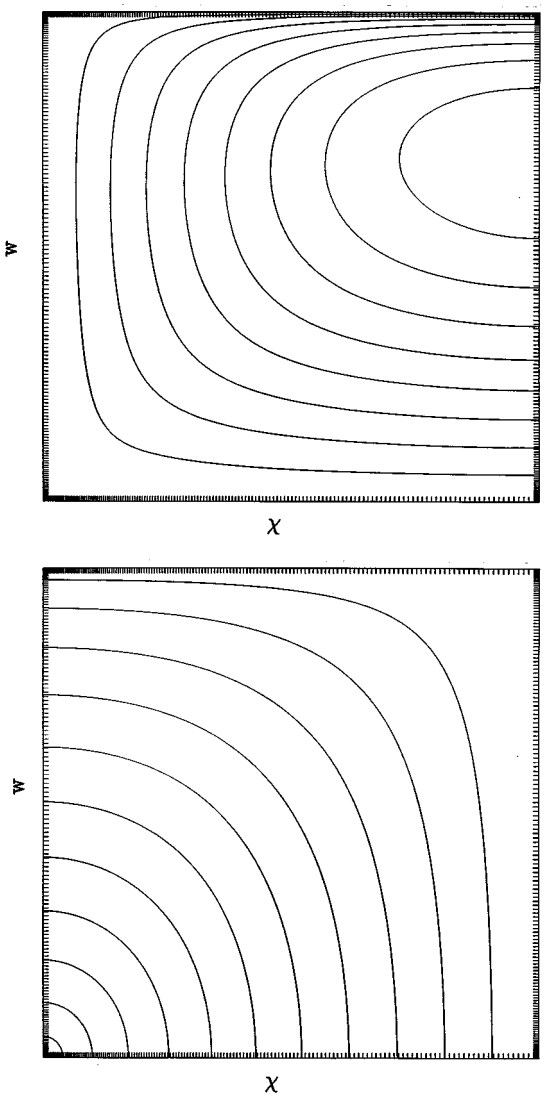

FIG. 13. Isocontour patterns in the (χ,w) plane of the functions (a) ϕ_1 and (b) ϕ_2 solutions of the K model in three dimensions with $\alpha=0.7$ ($\lambda=1.375$). The contour intervals are 2×10^{-2} (a) and 10^{-1} (b).

$$\tilde{a}_q^{\,+}(w)\equiv w^2\partial_w[(1-w^2)\partial_w a_q^+(w)]-\frac{w^2}{4}\frac{q^2+1}{1-w^2}a_q^+(w)-\frac{wq}{2(1-w^2)}a_q^+(w), \quad (26a)$$

$$\tilde{a}_q^{\,-}(w)\equiv w^2\partial_w[(1-w^2)\partial_w a_q^-(w)]-\frac{w^2}{4}\frac{q^2+1}{1-w^2}a_q^-(w)+\frac{wq}{2(1-w^2)}a-_q(w). \quad (26b)$$

Finally, perturbation theory [21] suggests that at leading order, only the product $m\times q$ matters, so it seems appropriate to investigate the ratios $\tilde{a}_q^{\pm}(w)/a_q^{\pm}(w)$. In the case of the Batchelor-Kraichnan operator, these two ratios are equal to 3/4. If the correlation function were to remain an eigenfunction of G^2, there ratios would remain constant.

Figure 15 shows the ratios $\tilde{a}_q^{\,+}(w)/a_q^+(w)$ (full line) and $\tilde{a}_q^{\,-}(w)/a_q^-(w)$ (dashed line) for $q=3$ as a function of w for

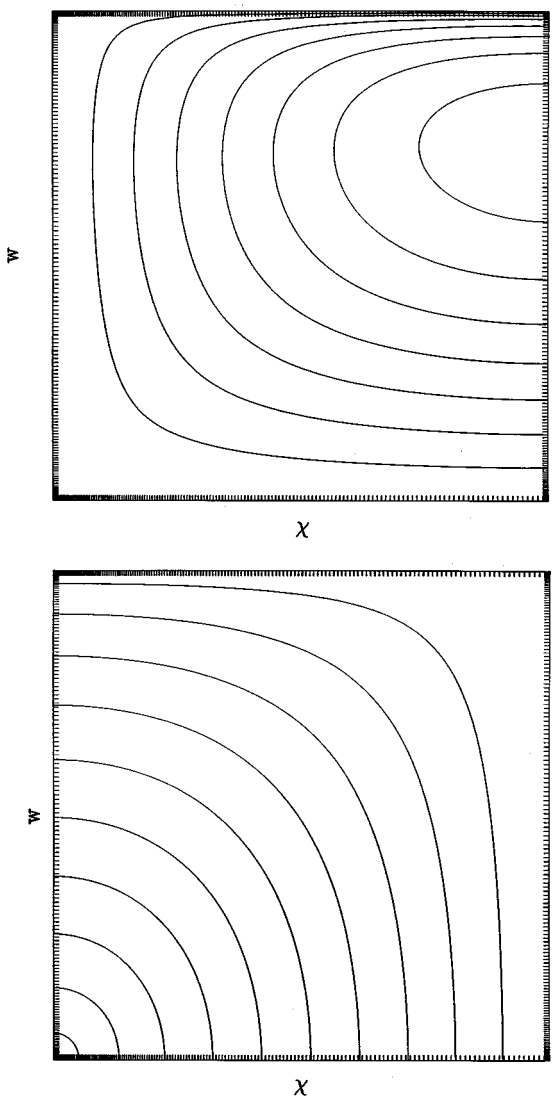

FIG. 14. Isocontour patterns in the (χ,w) plane of the functions (a) ϕ_1 and (b) ϕ_2 solutions of the white-noise problem in three dimensions with $\epsilon=\frac{2}{3}$ ($\lambda=1.380$). Observe the very close similarity to Fig. 13. The contour intervals are 2×10^{-2} (a) and 10^{-1} (b).

the solution of the K model for $\alpha=0.025$, 0.1, and 0.4. For $\alpha=0.025$ and 0.1, these functions show a sharp variation near $w=0$ and a more gentle variation away from $w=0$. The variation is sharper as α gets smaller, in agreement with the perturbation theory, which predicts a boundary layer width of size $\alpha^{1/2}$. When $\alpha=0.4$, the ''boundary layer'' is so thick that it extends very far away from $w=0$. As α decreases, the ratios $\tilde{a}_3^{\pm}(w)/a_3^{\pm}(w)$ are very close to 3/4, as expected for the zero modes of the Batchelor-Kraichnan operator.

Away from the boundary layer near $w=0$, the values of $\tilde{a}_3^{\pm}(w)/a_3^{\pm}(w)-3/4$ grow roughly linearly with α. To understand this phenomenon, we begin by recalling that away from $w=0$, the solution is close to a solution of the Batchelor-Kraichnan operator. The $q=\pm3$ component of the solution is therefore close to the eigenmode given by Eq. (16), with $\nu=1/2$, $\lambda=1$, $m=\pm1$, and $q=\pm3$, and referred to here for simplicity as ψ_0. A formal perturbation theory in the form $\psi\equiv\psi_0+\alpha\psi_1+O(\alpha^2)$, valid away from $w=0$, may be constructed. Standard perturbation theory then leads to $(G^2-3/4)\psi_1=-L_D\psi_0$, which implies that $\tilde{a}_3^{\pm}(w)/a_3^{\pm}(w)-3/4\alpha(L_D\psi_0)^{\pm}/a_3^{\pm}(w)+O(\alpha^2)$, consistent with the numerical results.

The ratios $\tilde{a}_q^{\pm}(w)/a_q^{\pm}(w)$ for higher values of q ($q=9,15,...$) show a qualitatively similar behavior. As the value of q becomes larger, however, the ratios determined numerically are further away from the value 3/4, corresponding to the Batchelor-Kraichnan operator.

It results from Fig. 15 that the SL(2) symmetry, as measured by the ratios $\tilde{a}_q^{\pm}(w)/a_q^{\pm}(w)$, is significantly affected by the perturbation term, even for very small values of α. The same conclusion is true for the white-noise problem. In particular, the SL(2) symmetry is completely lost when $\epsilon=2/3$ in this sense.

The conclusion of this subsection is that the SL(2) symmetry is presumably very difficult to check directly, at least by using directly the G^2 operator. This can be understood since G^2 is a second-order operator, which tends to amplify the differences greatly. The results presented here are much less favorable that the direct comparison with the integral representation, presented in Sec. III E. As a consequence, it seems very unlikely that one will be able to check directly the SL(2) symmetry directly from experimental data. A comparison with the integral representation appears to be more appropriate.

V. CONCLUDING REMARKS

We have presented a detailed numerical investigation of two classes of approximate models, introduced to describe turbulent advection. Mathematically the study of the three-point correlation function, in the presence of an external gradient and for these models, can be formulated as an elliptic (nonlinear) eigenvalue problem. This problem can be treated numerically using standard routines and both the exponent and the full correlation function can be determined.

One important conclusion is that our numerical results generally confirm all the available theoretical predictions. In particular, the fairly sophisticated asymptotic calculation near the Batchelor limit captures well the features of the numerical solution. In particular, close to $\alpha=0$ in the K model, the exponent remains close to 1: $\delta\equiv\lim_{\alpha\to0}(\lambda-1)/\alpha=0$. The same behavior has been found in the white-noise problem.

As expected from perturbation theory, several important properties of the correlation function can be deduced from the value of δ. The Batchelor-Kraichnan operator is infinitely degenerate and the perturbation term lifts the degeneracy and effectively determines the solution by selecting the combination of modes (selection of the correlation function). This property is expressed by the integral representation (20) and (21). We have found that the solution is indeed very well represented by the integral representation, a nontrivial result since it expresses the solution of the elliptic problem as an elementary integral. Once again, the results are very similar for the K model and for the white-noise problem. In a way we do not understand at the moment, these results suggest a universality of the solution of the problem near the Batchelor limit.

This study was intended to investigate the persistence of a small-scale anisotropy in the mixing of a passive scalar in

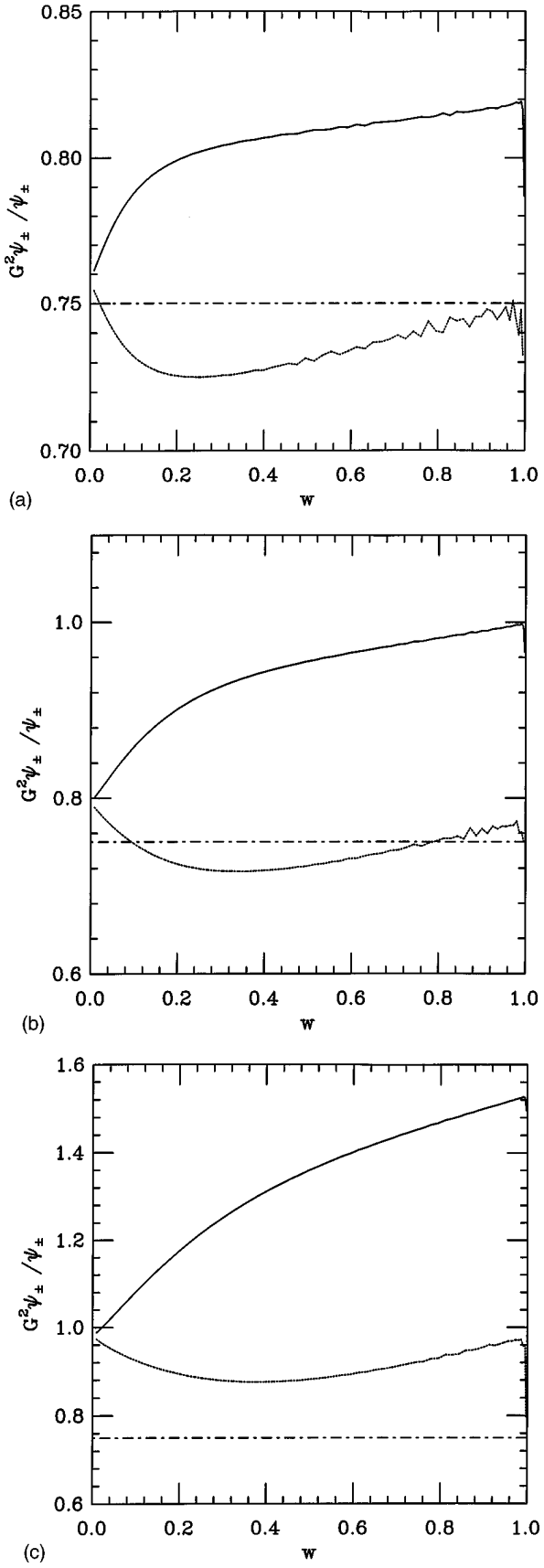

FIG. 15. Ratios $\widetilde{a}_q(w)/a_q(w)$ (full line) and $\widetilde{b}_q(w)/b_q(w)$ ($q=3$) as functions of w for the solution of the K model of $\alpha=0.025$ (a), 0.1 (b), and 0.4 (c). As α increases, these ratios are further away from a constant value, showing that the G^2 symmetry is lost.

the presence of an external gradient. The fact that the exponent observed experimentally is approximately equal to 1 suggests that a small value of α or ϵ has to be chosen in order to compare experiments with the predictions of the model. The value of the exponent for the white-noise problem with $\epsilon=2/3$ is $\lambda\approx 1.38$, much larger than what is found experimentally. This suggests that the predictions of the white-noise model cannot precisely describe the experimental results. The complete determination of the three-point correlation function allows one to compare the results of the model with direct experimental measurements and thus to gauge the validity of the K model.

ACKNOWLEDGMENTS

It is a pleasure to thank B. Shraiman and E. Siggia, who shared very generously their insight with me. This work was initiated during a visit to Cornell University. The financial support from DRET, under Contract No. 95-2591A, is acknowledged.

APPENDIX A

In this appendix we give the explicit form of the differential operators studied numerically in our variables (χ,w), in two dimensions. In the following, I is the identity matrix and σ_x and σ_z the Pauli matrices $\sigma_x\equiv\left(\begin{smallmatrix}0&1\\1&0\end{smallmatrix}\right)$ and $\sigma_z\equiv\left(\begin{smallmatrix}1&0\\0&-1\end{smallmatrix}\right)$. The function $\beta(\chi)$ is defined by

$$\beta(x)=([1-\sqrt{1-w^2}\,\cos(2\chi)]\times\{1-\sqrt{1-w^2}\,\cos[2(\chi+2\pi/3)]\}\times\{1-\sqrt{1-w^2}\,\cos[2(\chi-2\pi/3)]\})^{2/3}, \quad \text{(A1)}$$

1. *K*-model in two dimensions

$$A_{ww}=(1-w^2)[w^2+\alpha\beta(\chi)]\times I, \quad \text{(A2)}$$

$$A_{\chi\chi}=[w^2+\alpha\beta(\chi)]/(1-w^2)\times\frac{I}{4}, \quad \text{(A3)}$$

$$A_{\chi w}=0, \quad \text{(A4)}$$

$$A_{\chi}=w/(1-w^2)[1+\alpha\beta(\chi)]\sigma_x/2, \quad \text{(A5)}$$

$$A_w=\{[(\lambda-2)w^2-\lambda]w-2\alpha\beta(\chi)w\}\times I, \quad \text{(A6)}$$

$$A=[(2\lambda-\lambda^2)w^2+(\lambda-1)(\lambda+3)+\alpha\beta(\chi)(2\lambda+\lambda^2)]\times\frac{I}{4}. \quad \text{(A7)}$$

2. White-noise problem in two dimensions

$$A_{ww}=(\tfrac{2}{3}(3-\epsilon)w(1-w^2)\{[1-\sqrt{1-w^2}\,\cos(2\chi)]/w\}^{1-\epsilon/2}$$
$$-\tfrac{1}{3}(2-\epsilon)w^2(1-w^2)[1+2\cos(4\chi)]\{[1-\sqrt{1-w^2}\,\cos(2\chi)]/w\}^{-\epsilon/2}+\cdots)\times I, \tag{A8}$$

$$A_{\chi\chi}=\left(\frac{(3-\epsilon)w}{6(1-w^2)}[1+2\sqrt{1-w^2}\,\cos(2\chi)]\{[1-\sqrt{1-w^2}\,\cos(2\chi)]/w\}^{1-\epsilon/2}\right.$$
$$\left.-\frac{2-\epsilon}{12(1-w^2)}[w^2-2\cos(4\chi)+2\sqrt{1-w^2}\,\cos(2\chi)]\{[1-\sqrt{1-w^2}\,\cos(2\chi)]/w\}^{-\epsilon/2}+\cdots\right)\times I, \tag{A9}$$

$$A_{\chi}=\left(\frac{2\lambda(3-\epsilon)w}{3\sqrt{1-w^2}}\cos(2\chi)\{[1-\sqrt{1-w^2}\,\cos(2\chi)]/w\}^{1-\epsilon/2}+\frac{2-\epsilon}{6(1-w^2)}\{[4(\lambda-1)-\lambda w^2]\sqrt{1-w^2}\,\sin(2\chi)+2[1-\lambda+(1\right.$$
$$\left.+\lambda)w^2]\sin(4\chi)\}\times\{[1-\sqrt{1-w^2}\,\cos(2\chi)]/w\}^{-\epsilon/2}+\cdots\right)\times I+\left(\frac{-(3-\epsilon)w^2}{3(1-w^2)}\{[1-\sqrt{1-w^2}\,\cos(2\chi)]/w\}^{1-\epsilon/2}\right.$$
$$\left.+\frac{(2-\epsilon)w}{6(1-w^2)}\{[1-\sqrt{1-w^2}\,\cos(2\chi)]/w\}^{-\epsilon/2}[-\sqrt{1-w^2}\,\cos(2\chi)+2\cos(4\chi-1)]+\cdots\right)\times\sigma_x, \tag{A10}$$

$$A_{\chi w}=-\frac{(2-\epsilon)w}{3}(\{[1-\sqrt{1-w^2}\,\cos(2\chi)]/w\}^{-\epsilon/2}[2\sin(2\chi)-\sqrt{1-w^2}\,\sin(4\chi)]+\cdots), \tag{A11}$$

$$A_{w}=(\tfrac{4}{3}(3-\epsilon)w^2\{[1-\sqrt{1-w^2}\,\cos(2\chi)]/w\}^{1-\epsilon/2}\times[-1+(\lambda-2)\sqrt{1-w^2}\,\cos(2\chi)]$$
$$-w(2-\epsilon)/3\{[1-\sqrt{1-w^2}\,\cos(2\chi)]/w\}^{-\epsilon/2}\times\{2(2-\lambda)(1-w^2)\cos(4\chi)+\sqrt{1-w^2}(3\lambda-4)\cos(2\chi)$$
$$-[(2-\lambda)w^2+\lambda]\}+\cdots)\times I+(-\tfrac{4}{3}(3-\epsilon)w\sqrt{1-w^2}\{[1-\sqrt{1-w^2}\,\cos(2\chi)]/w\}^{1-\epsilon/2}\sin(2\chi)$$
$$+\tfrac{2}{3}(2-\epsilon)w^2\{[1-\sqrt{1-w^2}\,\cos(2\chi)]/w\}^{-\epsilon/2}\sin(4\chi)+\cdots)\times\sigma_x, \tag{A12}$$

$$A=\left(-\frac{(3-\epsilon)w}{6(1-w^2)}\{[1-\sqrt{1-w^2}\,\cos(2\chi)]/w\}^{1-\epsilon/2}[1-2\cos(2\chi)\sqrt{1-w^2}]\right.$$
$$+\frac{(3-\epsilon)w}{6}\{[1-\sqrt{1-w^2}\,\cos(2\chi)]/w\}^{1-\epsilon/2}[2\lambda+\lambda^2+2\sqrt{1-w^2}(2\lambda-\lambda^2)\cos(2\chi)]$$
$$+\frac{(2-\epsilon)w^2}{12(1-w^2)}\{[1-\sqrt{1-w^2}\,\cos(2\chi)]/w\}^{-\epsilon/2}[1-2\cos(4\chi)]-(2-\epsilon)/12\{[1-\sqrt{1-w^2}\,\cos(2\chi)]/w\}^{-\epsilon/2}$$
$$\left.\times[2(1-w^2)(\lambda^2-2\lambda)\cos(4\chi)+\sqrt{1-w^2}\,\cos(2\chi)(8\lambda-6\lambda^2)+w^2(2\lambda-\lambda^2)+4(\lambda^2-\lambda)]+\cdots\right)$$
$$\times I-\left(\frac{2(3-\epsilon)w^2\lambda}{3\sqrt{1-w^2}}\sin(2\chi)\{[1-\sqrt{1-w^2}\,\cos(2\chi)]/w\}^{1-\epsilon/2}-\frac{(2-\epsilon)w}{6(1-w^2)}\{[1-\sqrt{1-w^2}\,\cos(2\chi)]/w\}^{-\epsilon/2}\right.$$
$$\left.\times\{[2\lambda(1-w^2)-4]\sin(4\chi)+\sqrt{1-w^2}\,(4-3\lambda)\sin(2\chi)\}+\cdots\right)\times\sigma_x. \tag{A13}$$

APPENDIX B

In this appendix we give the expression of the solution near the point $\vec{\rho}_1=0$. Without loss of generality, we take $\xi_2=1$ and introduce the variable $u=2\chi$. Physically, u is the coordinate of $\vec{\rho}_1$ along the axis parallel to $\vec{\rho}_2$, whereas w is the distance to the origin in the plane perpendicular to $\vec{\rho}_2$ [the norm of $\vec{\rho}_1$ is denoted as ρ, with $\rho\equiv\frac{1}{2}(u^2+w^2)^{1/2}$]. This interpretation suggests the use of also spherical coordinates $u=\rho\cos\theta$ and $w=\rho\sin\theta$.

For the K model, in three dimensions, the equations reduce in the limit $|\rho_1|\to 0$ to

$$\left(\frac{9}{8}\right)^{2/3}\alpha(u^2+w^2)^{2/3}\left[\partial_w^2+\partial_u^2+\frac{1}{w}\,\partial_w-\frac{1}{w^2}\begin{pmatrix}1&0\\0&0\end{pmatrix}\right]\begin{pmatrix}\phi_1\\\phi_2\end{pmatrix}$$
$$=-\left[w^2(\partial_w^2+\partial_u^2)-w\partial_w+\begin{pmatrix}0&1\\-1&0\end{pmatrix}\partial_u+\frac{5}{3}(\lambda-1)\right]\times\begin{pmatrix}\phi_1\\\phi_2\end{pmatrix}. \tag{B1}$$

When $\lambda=1$, $(\phi_1,\phi_2)=(0,-1)$ is a solution (zeroth order). A systematic expansion can thus be generated by simply plugging in the $(n-1)$th order on the right-hand side of Eq. (A1) and solving the inhomogeneous equation to determine the nth order. The expansion is formally valid provided $u^2+w^2\ll\alpha^3$. The first orders determined in this way are

$$\begin{pmatrix}\phi_1\\\phi_2\end{pmatrix}=\begin{pmatrix}0\\-1\end{pmatrix}+\delta(\alpha)(2\rho)^{2/3}\begin{pmatrix}f_1(\overline{\rho},\theta)\\f_2(\overline{\rho},\theta)\end{pmatrix}, \tag{B2}$$

with $\delta(\alpha)\equiv(\frac{8}{9})^{2/3}(\lambda-1)/\alpha$ and $\overline{\rho}\equiv\rho/\alpha^{3/2}$, and

$$f_1(\overline{\rho},\theta)=+\tfrac{9}{26}\,\delta(\alpha)(2\overline{\rho})^{2/3}\sin\theta\cos\theta+O(\overline{\rho}^{4/3}), \tag{B3}$$

$$f_2(\overline{\rho},\theta)=+\tfrac{3}{2}-\{[\tfrac{45}{56}\,\delta(\alpha)\alpha-\tfrac{27}{182}]+\tfrac{3}{26}\sin^2\theta\}\overline{\rho}^{2/3}+O(\overline{\rho}^{4/3}). \tag{B4}$$

These results suggest that the solution is made of an s-wave piece (independent of θ) that behaves as $1+O(\rho^{2/3})$, provided $\delta\neq 0$, plus a d-wave piece (with an angular dependence approximately equal to $\sin 2\theta$ or $\cos 2\theta$) that depends on ρ like $\rho^{4/3}$. An unpleasant feature of our model is that it is not possible to determine unambiguously higher-order terms in $\overline{\rho}^{2/3}$ since terms such as $\binom{\rho^2\sin\theta\cos\theta}{0}$ are zero modes of the Laplacian operator on the left-hand side of Eq. (B1).

APPENDIX C

We estimate here the integral representation near the point $(\chi,w)=(0,0)$. We restrict ourselves to the case considered here, where the coefficient $f_{2/3}=0$ (the function f has a $\chi/|\chi|^2$ singularity).

Our starting point is the integral representation, which can be expressed in the form (when χ and w are small, and in the limit $\lambda-1\to 0$)

$$\Psi=\hat{G}\int_0^{2\pi}[w/2\,\hat{\eta}_1+(\chi-\phi)\,\hat{\eta}_2]\times\ln[w^2/4+(\chi-\phi)^2]f(\phi)d\phi. \tag{C1}$$

(we have taken $\xi_2=1$). This integral is to be understood as a principal value near $\phi=0$.

The integral (C1) can be rewritten in complex notation. Introducing the variable $z=iw/2+\chi$ (with z^* its complex conjugate), the real and imaginary parts of

$$\Psi'=i\int_0^{2\pi}(z^*-\phi)\ln|z-\phi|^2 d\phi \tag{C2}$$

are, respectively, the ϕ_1 and ϕ_2 components of the solution. Differentiating Eq. (C2) with respect to z and then with respect to z^*, one obtains

$$\partial_z\partial_{z^*}\Psi'=\int_0^{2\pi}\frac{f(\phi)d\phi}{(z-\phi)}, \tag{C3}$$

which can be evaluated by elementary methods

$$\partial_z\partial_{z^*}\Psi'=\pi\,\frac{\mathrm{Im}(z)}{z}. \tag{C3a}$$

Similarly, one obtains

$$\partial_{z^*}^2\Psi'=-\pi\,\frac{\mathrm{Im}(z)}{z^*} \tag{C3b}$$

and

$$\partial_z\Psi'=\pi\,\frac{\mathrm{Im}(z)}{z}\,(z^*-z). \tag{C3c}$$

Integrating Eqs. (C1)–(C3), one obtains

$$\Psi'=\pi\,\mathrm{Im}(z)\left[z^*\ln\left(\frac{z}{z^*}\right)+z^*-z\right]. \tag{C4}$$

Defining $\theta=\arctan(w/2\chi)$, one obtains Eq. (24).

[1] K. R. Sreenivasan, Proc. R. Soc. London, Ser. A **434**, 165 (1991).
[2] A. N. Kolmogorov, Dokl. Akad. Nauk SSSR **30**, 301 (1941).
[3] U. Frisch, *Turbulence: The Legacy of A. N. Kolmogorov* (Cambridge University Press, Cambridge, 1995).
[4] A. M. Obukhov, Izv. Akad. Nauk SSSR, Geogr. Geophys. Ser. **13**, 58 (1949).
[5] S. Corrsin, J. Appl. Phys. **22**, 469 (1951).
[6] C. Tong and Z. Warhaft, Phys. Fluids **6**, 2165 (1994); L. Mydlarski and Z. Warhaft, J. Fluid Mech. (to be published).
[7] R. Antonia *et al.*, Phys. Rev. A **30**, 5 (1984).
[8] P. Mestayer, J. Fluid Mech. **125**, 475 (1982).
[9] R. A. Antonia and C. W. Van Atta, J. Fluid Mech. **84**, 561 (1980).
[10] C. Tong and Z. Warhaft, Phys. Fluids **6**, 2165 (1994).
[11] M. Holzer and E. D. Siggia, Phys. Fluids **6**, 1820 (1994).
[12] A. Pumir, Phys. Fluids **6**, 2118 (1994).
[13] R. H. Kraichnan, Phys. Fluids **11**, 945 (1968).
[14] B. I. Shraiman and E. D. Siggia, Phys. Rev. E **49**, 2912 (1994).
[15] M. Chertkov *et al.*, Phys. Rev. E **52**, 4924 (1995).

[16] K. Gawędzki and A. Kupiainen, Phys. Rev. Lett. **75**, 3834 (1995).
[17] B. I. Shraiman and E. D. Siggia, C. R. Acad. Sci. **321**, 279 (1995).
[18] B. I. Shraiman and E. D. Siggia, Phys. Rev. Lett. **77**, 2463 (1996).
[19] G. K. Batchelor, J. Fluid Mech. **5**, 113 (1959).
[20] A. Pumir, B. I. Shraiman, and E. D. Siggia, Phys. Rev. E **55**, 1263 (1997).
[21] B. I. Shraiman and E. D. Siggi, Phys. Rev. E **57**, 2965 (1998).
[22] A. Pumir, Europhys. Lett. **37**, 529 (1997).
[23] E. Balkovsky, M. Chertkov, I. Kolokolov, and V. Lebedev, Pis'ma Zh. Eksp. Teor. Fiz. **61**, 1049 (1995) [JETP Lett. **61**, 1012 (1995)].
[24] A. Pumir, Europhys. Lett. **34**, 25 (1996).
[25] D. Gutman and E. Balkovsky, Phys. Rev. E **54**, 4435 (1996).
[26] W. H. Press *et al.*, *Numerical Recipes* (Cambridge University Press, Cambridge, 1988).